Excitation migration in trimeric cyanobacterial photosystem I[a]

Melih K. Şener
Beckman Institute, University of Illinois at Urbana-Champaign, Urbana, Illinois 61801

Sanghyun Park and Deyu Lu
Beckman Institute, University of Illinois at Urbana-Champaign, Urbana, Illinois 61801 and Department of Physics, University of Illinois at Urbana-Champaign, Urbana, Illinois 61801

Ana Damjanović
Department of Biophysics, Johns Hopkins University, Maryland 21218

Thorsten Ritz
Department of Physics and Astronomy, University of California, Irvine, California 92697

Petra Fromme
Department of Chemistry and Biochemistry, Arizona State University, Tempe, Arizona 85287

Klaus Schulten[b]
Beckman Institute, University of Illinois at Urbana-Champaign, Urbana, Illinois 61801 and Department of Physics, University of Illinois at Urbana-Champaign, Urbana, Illinois 61801

A structure-based description of excitation migration in multireaction center light harvesting systems is introduced. The description is an extension of the sojourn expansion, which decomposes excitation migration in terms of repeated detrapping and recapture events. The approach is applied to light harvesting in the trimeric form of cyanobacterial photosystem I (PSI). Excitation is found to be shared between PSI monomers and the chlorophylls providing the strongest respective links are identified. Excitation sharing is investigated by computing cross-monomer excitation trapping probabilities. It is seen that on the average there is a nearly 40% chance of excitation cross transfer and trapping, indicating efficient coupling between monomers. The robustness and optimality of the chlorophyll network of trimeric PSI is examined. © *2004 American Institute of Physics.*
[DOI: 10.1063/1.1739400]

I. INTRODUCTION

As the main source of energy for life on earth, photosynthetic systems display a wide variety of structural motifs.[1,2] A common theme found in all photosynthetic systems, from the evolutionarily simpler[3,4] and anoxygenic light harvesting apparatus found in purple bacteria[5–8] to the more complex light harvesting systems used in oxygenic photosynthesis,[9–11] is the presence of pigment antenna complexes delivering the absorbed light energy to a reaction center for charge transfer. Recently, light harvesting supercomplexes comprised of various core subunits were discovered in oxygenic photobacteria.[12–15] These supercomplexes contain multiple reaction centers, as well as surrounding antenna systems consisting of several hundred chlorophylls, thus constituting new challenges to the modelling of the excitation migration process. In this paper we develop a framework for modelling excitation migration and connectivity in a light harvesting system consisting of multiple protein–pigment complexes and reaction centers. We apply this framework to the trimeric form of cyanobacterial photosystem I (see Fig. 1), and seek an answer to the question why nature builds coupled multimeric units as opposed to independent ones.

In oxygenic species, such as plants, algae, and cyanobacteria, the first step of energy transformation, the capture of light followed by a transmembrane charge separation, is performed by two large membrane proteins, photosystem I (PSI) and photosystem II (PSII). The 2.5 Å resolution structure for the PSI complex from the cyanobacterium *Synechococcus (S.) elongatus*[9] reveals 96 chlorophylls and 22 carotenoids comprising an antenna array. A peculiar feature of cyanobacterial PSI is its occurrence in both monomeric and trimeric forms depending on growth conditions. This is in contrast to plant PSI, which is observed only in monomeric form. Mutagenesis studies on deletion mutants of PsaL (a protein subunit of PSI featuring transmembrane α-helices, located at the trimer interface) in *S. elongatus* have shown that the trimerization is essential for the growth of the cells at low light intensity[16,17] (which corresponds to the light intensity in the natural habitat). In case of iron deficiency, cyanobacterial PSI is known to arise in the form of supercomplexes comprised of a trimeric PSI core surrounded by eighteen IsiA (a CP43-like iron stress-induced protein) satellite complexes.[12,13] In such a complex nearly 500 chlorophylls surround three reaction centers. Similar complexes have also been reported for PSII.[15] The surrounding satellite complexes appear to serve the purpose of increasing the total absorption cross section, thereby increasing the light harvesting capacity of the core complex significantly. In fact,
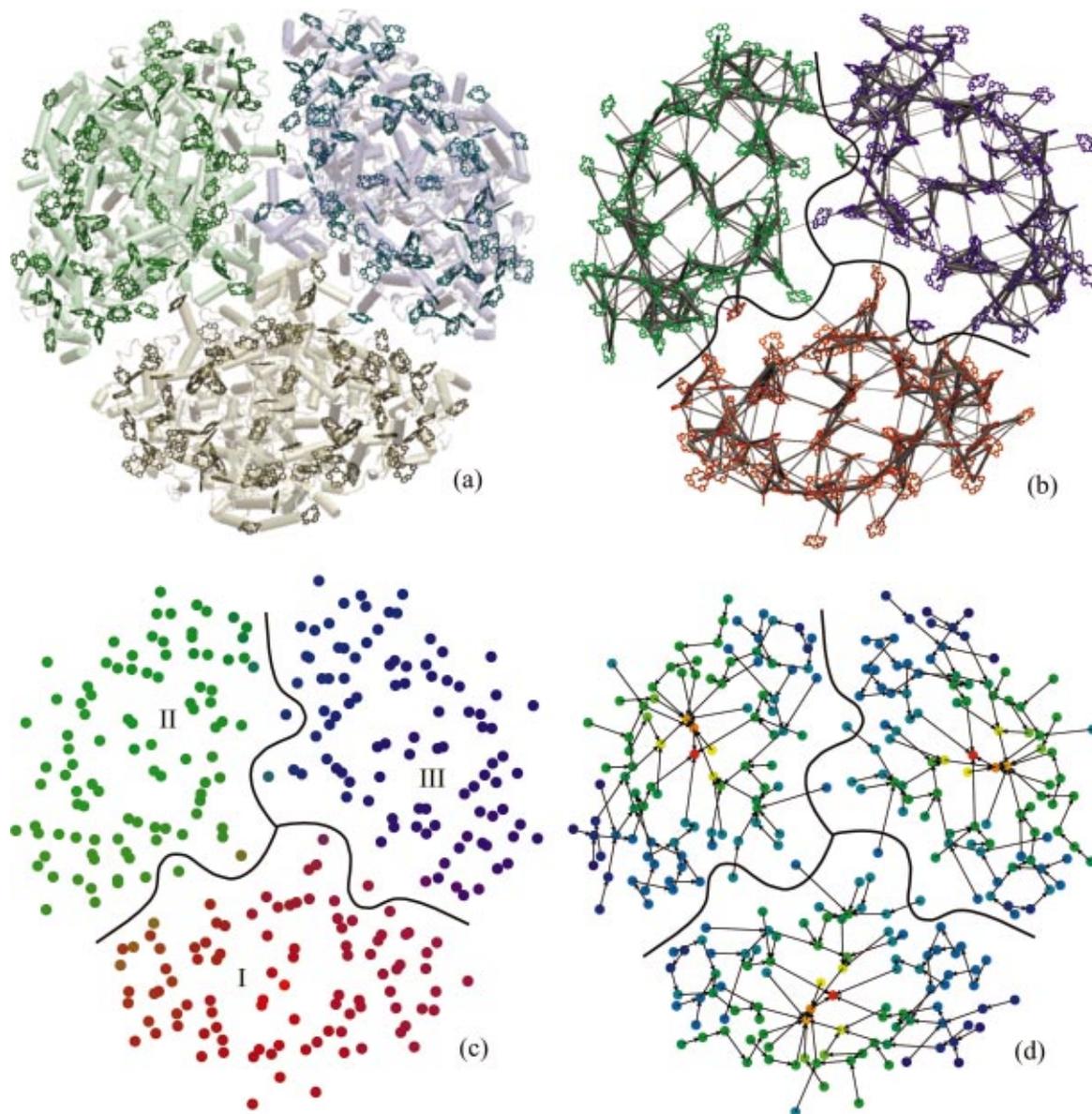
FIG. 1. (Color) Chlorophyll network of trimeric PSI from cyanobacterium *S. elongatus*. (a) The trimeric protein–pigment complex. For simplicity, cofactors other than chlorophylls are not shown. Different monomers and their chlorophylls are depicted in different colors. (b) Excitation transfer rates between individual chlorophylls. The thickness of a bond between two chlorophylls is proportional to the logarithm of the transfer rate between them. For simplicity, only the largest rates are shown. (c) Connectivity between different monomers. The measure is given by the probabilities of charge transfer from a given reaction center for an initial condition corresponding to a perfectly localized excitation at a given chlorophyll. The content of red, green, and blue are proportional to the probability of charge transfer from the bottom, left and right reaction centers, respectively (see also Fig. 4). (d) Excitation migration. The arrows between chlorophylls characterizing the migration are assigned according to the steepest-descent criterion based on mean first passage times to the reaction centers (see text). The colors denote increasing mean first passage times from red to blue. (a) and (b) were produced with VMD (Ref. 57).

Melkozernov *et al.*[18] have recently reported that there is efficient energy transfer from the IsiA antenna ring to the PSI core.

The existence of light harvesting systems comprised of multiple integrally connected protein–pigment complexes brings up questions regarding the degree of connectivity between individual subunits, as well as the rationale behind the formation of multimeric units. The case of peripheral antenna rings surrounding a reaction center core through an efficient coupling is self-explanatory, as this increases the overall absorption cross section. However, it is less obvious what advantage is gained by the formation of a trimeric PSI complex as opposed to having three separate monomers. Can

this be explained solely in the context of excitation transfer dynamics or does the reason of trimer formation lie with a different aspect of the light harvesting function? The question why PSI forms trimers in cyanobacteria is an exciting and controversial issue and there is a great need for experimental evidence concerning the function of the trimerization. As a first step in answering the questions raised by trimer formation in PSI, we perform a theoretical study of the excitation transfer dynamics in the trimeric form of PSI, specifically investigating the degree of connectivity between individual monomers.

Excitation transfer dynamics in PSI has been the subject of much theoretical and experimental study,[19–27] as well as

reviews.[28–30] With the availability of a high resolution structure[9] for PSI an opportunity arises to explore the excitation transfer dynamics at a level of detail hitherto not possible. The earliest such studies[31,32] concentrated on the nature of the chlorophyll network of PSI, 96 chlorophylls, with no apparent symmetry, providing challenges not seen in the cylindrically symmetrical chlorophyll aggregates of purple bacteria.[33,34] The computation of chlorophyll site energies[35] proves to be a crucial step in any detailed modelling effort. In the earlier work[32] we have discovered a high degree of robustness of PSI light harvesting and examined the degree of its optimality. The light harvesting function of PSI was found to be robust against thermal fluctuations of chlorophyll site energies as well as against the pruning of individual chlorophylls. This study was based on an effective Hamiltonian model and an application of Förster theory. A more recent study by Yang *et al.*,[36] in the context of a Redfield theory approach, identifies the rate determining steps in excitation transfer and discusses the role of individual chlorophyll groups, such as linker chlorophylls, on the excitation migration process. A recent comparison of Redfield and Förster theories in the context of excitation transfer dynamics can be found in Ref. 37. Successive kinetic domains in PSI, along which excitation migration proceeds, have been discussed in Ref. 38.

Even with the availability of a high resolution structure, many questions about the light harvesting function of PSI remain unanswered. One such question regards the nature of the so-called red chlorophyll states observed in the absorption spectrum of PSI, corresponding to chlorophylls that apparently absorb light at longer wavelengths than P700.[21,27] It has been argued that the main function of the red chlorophylls is to extend the absorption profile of PSI. The red chlorophyll states contribute significantly to the overall light harvesting capacity of PSI. An attempt to assign red chlorophyll states based on the strength of excitonic couplings alone without regard to chlorophyll site energies proves unsatisfactory.[32] The low temperature absorption spectrum based on a computation of chlorophyll site energies[35] successfully reproduces the width of the main absorption peak corresponding to bulk chlorophylls, but not the details of the red chlorophyll band. The spatial assignment of the red chlorophyll states remains yet to be established.

Another issue yet unresolved concerns the directionality of the electron transfer chain in PSI. Electron transfer chains in reaction center cores have a conserved structural motif consisting of two bifurcating paths of electron carriers. In case of purple bacteria, the nature of the charge transfer has been studied in great detail.[39–41] In purple bacteria only one of the two branches is active, whereas in the case of PSI the question of whether one or both of the branches performs electron transfer is an open question. Evidence has been provided for both unidirectional[42–44] and bi-directional[45,46] electron transfer scenarios. It is possible that both branches are active with one of them being predominant. The results differ in cyanobacteria and green algae. Whereas the studies on the cyanobacterial system suggest the A-branch as the only active branch,[43,44] there is evidence from the studies on the green algae *Chlamydomonas rheinhardtii* that both branches

may be active with the B-branch being the faster and more important branch.[45–47] Therefore, the pathway of electrons may differ in green algae and cyanobacteria.

The question of whether two branches or only one branch is active, is difficult to answer at the present state of knowledge. Since we are working with the structure of a cyanobacterium, we will assume below that only one branch, namely the A-branch, is dominant.

The next question, which has to be addressed, is which molecule(s) perform the charge separation, i.e., correspond to P700*. In an earlier study[32] we have considered a model with two reaction center chlorophylls contributing to electron transfer. In this work we will follow an alternative suggestion[36] in assuming that the charge separation may start from the chlorophyll a′ (eC-A1, corresponding to chlorophyll number 1; all nomenclature and chlorophyll orderings refer to Ref. 9 and the associated PDB structure file 1JB0), the A-branch chlorophyll of P700.

With the stated assumptions, a kinetic model of light harvesting in trimeric PSI can be established. This will be done in the present paper based on the structure revealed in Ref. 9. Structure-based models are built on the observed geometry of the chlorophyll ensemble and on *a priori* established physical properties of chlorophylls, i.e., they have no parameters chosen *a posteriori*, permitting one thereby to test our present understanding of the physics of light harvesting. Despite the seeming complexity of structure-based models, e.g., compared to schematic lattice models as reviewed in Ref. 48, one can actually achieve, even for the 288 chlorophyll trimeric PSI, through the sojourn expansion a simple and transparent decomposition of the overall light harvesting process in terms of a few intuitive characteristics as will be demonstrated below.

The organization of this paper is as follows: In the next section we discuss the effective Hamiltonian formulation for trimeric PSI and the excitation transfer process in terms of a master equation. Section III presents a generalization of the sojourn expansion for a light harvesting system with an arbitrary number of reaction centers. In Sec. IV we apply the expansion method developed earlier to the excitation migration in trimeric PSI. Section V examines the connectivity between individual PSI monomers in a trimer. The issues of robustness and optimality of the chlorophyll network of PSI are addressed in Sec. VI, especially in regard to the role of excitation sharing between monomers. Section VII contains our conclusive remarks.

II. EFFECTIVE HAMILTONIAN FOR TRIMERIC PSI AND MASTER EQUATION FOR EXCITATION TRANSFER

Structural information provided by the 2.5 Å resolution structure of PSI[9] enables one to construct an effective Hamiltonian for the chlorophyll network using the Q_y-excited states of chlorophylls as a basis set. This effective Hamiltonian is used, following the examples in Refs. 8, 49, 50, 51, to describe the excitation transfer process through a related master equation for excitation migration via Förster theory or its generalization. This approach has been outlined also in a previous publication[32] for monomeric PSI which we follow

closely below. As discussed in Ref. 32, the approach taken does not account for the properties of red chlorophylls.[21,27]

Each monomer of PSI contains $N=96$ chlorophylls. The chlorophyll ensemble of the trimer is depicted in Fig. 1. Its effective Hamiltonian is

$$
H = \begin{pmatrix}
\epsilon_1 & H_{12} & \cdots & H_{1,3N} \\
H_{21} & \epsilon_2 & \cdots & H_{2,3N} \\
\cdots & \cdots & \cdots & \cdots \\
H_{3N,1} & H_{3N,2} & \cdots & \epsilon_{3N}
\end{pmatrix},
\tag{1}
$$

where the diagonal entries are the chlorophyll site energies and the off-diagonal entries are the couplings between chlorophlls. The site energies used in this paper are taken from Ref. 35 after being shifted by 848 cm^{-1} to reproduce the observed absorption peak for PSI. The interchlorophyll couplings are computed in the full Coulomb picture as outlined in the appendix of Ref. 32. Accordingly, the choice of H did not involve any free parameters, in particular, all chlorophyll–chlorophyll couplings H_{ij} were determined according to the available x-ray structure 1JB0.[9]

Once the couplings and the site energies are known, the excitation transfer between individual chlorophylls arises actually incoherently (for a discussion see, e.g., Ref. 52) and, in the present case, rate constants can be computed in the context of Förster theory.[53–55] The rate of transfer of excitation from chlorophyll i to chlorophyll j is accordingly

$$
T_{ij} = \frac{2\pi}{\hbar}|H_{ij}|^2 J_{ij}, \quad J_{ij} = \int S_i^D(E)S_j^A(E)dE,
\tag{2}
$$

where J_{ij} describes the coupling to vibrational degrees of freedom expressed as the overlap integral between the donor emission spectrum $S_i^D(E)$ and the acceptor absorption spectrum $S_j^A(E)$. The functional forms of $S_i^D(E)$ and $S_j^A(E)$ are given in Ref. 32 and involve a Stokes shift and a spectral width chosen uniformly as 160 cm^{-1} and 240 cm^{-1}, respectively.[56] Otherwise, there are no free parameters to be selected. Below we consider only the dynamics at room temperature and use the corresponding line shapes. Low temperature effects, in particular an emerging role of red chlorophylls, were discussed in Ref. 32.

The transfer rates computed from (2) can be used to construct a graphical representation of the network of connections between chlorophylls as shown in Fig. 1(b). The thickness of the bond between chlorophylls i and j is taken to be proportional to the larger of $\log(T_{ij})+c$ and $\log(T_{ji})+c$, where c is a small constant. Only the strongest connections are shown for simplicity.

A master equation for excitation migration can be constructed from the transfer rates T_{ij} given in (2). Let us denote by $p_i(t)$ the probability that chlorophyll i is electronically excited at time t. The rate of change of these occupation probabilities due to excitation transfer, dissipation, or charge separation (if i is a charge separation site) is

$$
\frac{d}{dt}|p(t)\rangle = K|p(t)\rangle,
\tag{3}
$$

$$
K_{ij} = T_{ji} - \delta_{ij}\left(k_{CS}\delta_{i,CS}+k_{diss}+\sum_k T_{ik}\right),
\tag{4}
$$

where k_{diss} denotes the dissipation rate (sum of the rates of internal conversion and fluorescence) assumed to be uniform across chlorophylls, and k_{CS} denotes the trapping rate at a charge transfer site; $\delta_{i,CS}$ is equal to one if i is a charge separation site and zero otherwise; specifically, $\delta_{i,CS}$ is equal to one for $i \in \{1,N+1,2N+1\}$ for the present model of trimeric PSI with $N=96$. A dissipation rate of $k_{diss}=1$ ns^{-1} and a charge separation rate of $k_{CS}=1$ ps^{-1} is assumed throughout this paper.[58–60] The assumption of a larger dissipation rate results in a slightly reduced quantum yield [cf. Eq. (28)].

The solution to the master equation (3) is given by

$$
|p(t)\rangle = e^{Kt}|p(0)\rangle,
\tag{5}
$$

from which the average excitation lifetime can be derived following Ref. 55. The probability that at time t there is still an excitation somewhere in the system is

$$
n(t) = \sum_i \langle i|p(t)\rangle = \langle \mathbf{1}|p(t)\rangle,
\tag{6}
$$

where $|i\rangle \equiv (\delta_{1i},\delta_{2i},\ldots,\delta_{3N,i})_{3N}$ and $|\mathbf{1}\rangle \equiv (1,\ldots,1)_{3N}$. The probability that the excitation disappears between t and $t+dt$ is given by $-(d/dt)n(t)dt$. Thus, the expectation value of the average excitation lifetime is

$$
\tau = -\int_0^\infty dt\, t\, \frac{d}{dt}n(t).
\tag{7}
$$

Integrating by parts and employing (5) along with the identity for a matrix K with negative eigenvalues,

$$
\int_0^\infty dt\, e^{Kt} = -K^{-1},
\tag{8}
$$

yields an exact expression for the average excitation lifetime

$$
\tau = -\langle \mathbf{1}|K^{-1}|p(0)\rangle.
\tag{9}
$$

The respective lifetime for an initial condition $|p(0)\rangle = |i\rangle$, τ_i, is also referred to as mean first passage time, if one chooses the charge separation rate k_{CS} very large.

Likewise, one can readily determine the quantum yield Q of charge separation in one of the reaction centers. Defining by CS the set of chlorophyll sites where charge separation takes place and the respective states as $|j\rangle$, $j \in$ CS one can write

$$
Q = \int_0^\infty dt\, k_{CS}\sum_{j \in CS} \langle j|p(t)\rangle.
\tag{10}
$$

Employing (5) and (8) this becomes

$$
Q = -k_{CS}\sum_{j \in CS} \langle j|K^{-1}|p(0)\rangle.
\tag{11}
$$

Comparison of (9) and (11) shows that matrix elements of K^{-1} define both lifetimes and quantum yields for the system described by (3).

A very intuitive picture of the excitation migration can be constructed from steepest-descent pathways for excitation transfer based on mean first passage times to any of the re-

action centers as depicted in Fig. 1(d). Following Ref. 61, let τ_i^{MFPT} denote the mean first passage time from chlorophyll i to a reaction center. Representative excitation migration pathways are then constructed by following a path of steepest descent along mean first passage times. Accordingly, a path [represented by an arrow in Fig. 1(d)] follows from a chlorophyll i to that chlorophyll j for which $T_{ij}(\tau_i^{\mathrm{MFPT}} - \tau_j^{\mathrm{MFPT}})$ is largest. Such pathways are always unidirectional and terminate at a reaction center. As each chlorophyll only connects unidirectionally to one other chlorophyll, this diagram is split naturally into three disjoint sets of chlorophylls. It is noteworthy that these sets do not coincide with the sets of chlorophylls belonging to PSI monomers as one can readily discern from Fig. 1(d) as well as from Fig. 3 discussed below.

III. A GENERALIZATION OF THE SOJOURN EXPANSION FOR AN ARBITRARY NUMBER OF REACTION CENTERS

In this section we present an expansion for the excitation migration process in terms of repeated detrapping events. For this purpose we develop a general method for expanding the average excitation lifetime (9) in terms of excitation migration, trapping, and repeated detrapping and retrapping events. This method is a generalization of the sojourn expansion, introduced in Ref. 32 for a single reaction center.

Let us consider an antenna complex consisting of n pigments and M charge transfer sites and let the matrix K describing excitation migration be defined as in (4). Following Ref. 32, we first separate from K the operator Δ that describes detrapping events from any of the charge separation sites

$$K \equiv \kappa + \Delta,$$
$$\Delta \equiv \sum_{k=1}^{n} \sum_{j \in CS} T_{jk} |k\rangle\langle j|. \tag{12}$$

It is useful to introduce the total detrapping rate $W_{D,j} = \sum_{k=1}^{n} T_{jk}$ from the charge separation site labeled by j and the corresponding transient state

$$|T_j\rangle = \frac{1}{W_{D,j}} \sum_{k=1}^{n} T_{jk} |k\rangle, \quad j \in CS, \tag{13}$$

which describes the distribution of occupation probabilities immediately following a detrapping event from the charge separation site j. Thus, the detrapping operator in (12) can be written

$$\Delta = \sum_{j \in CS} W_{D,j} |T_j\rangle\langle j|. \tag{14}$$

An expansion for the average excitation lifetime given in (9) can be obtained by noting

$$K^{-1} = (\kappa + \Delta)^{-1}$$
$$= \kappa^{-1} - \kappa^{-1} \Delta \kappa^{-1} + \kappa^{-1} \Delta \kappa^{-1} \Delta \kappa^{-1} - \dots . \tag{15}$$

Combining (9) and (15) yields a series

$$\tau = \tau_0 + \tau_1 + \tau_2 + \dots,$$
$$\tau_0 = -\langle \mathbf{1} | \kappa^{-1} | p(0)\rangle,$$
$$\tau_1 = \langle \mathbf{1} | \kappa^{-1} \Delta \kappa^{-1} | p(0)\rangle, \tag{16}$$
$$\tau_2 = -\langle \mathbf{1} | \kappa^{-1} \Delta \kappa^{-1} \Delta \kappa^{-1} | p(0)\rangle.$$

Comparison with (9) shows that the first term τ_0 can be interpreted as a first usage time, corresponding to the average excitation lifetime without any detrapping events. In general, this will be the mean first passage time to the charge separation site plus the charge separation time. Each successive term in the series (16) describes the contribution to the average excitation lifetime by processes involving an increasing number of detrapping events. The convergence of this expansion is proved below.

The various terms in the expansion (16) can be rewritten using (14). For this purpose, let us first note that the detrapping probability from the charge separation site j corresponding to an initial state $|S\rangle$ is

$$Q_S = -W_{D,j}\langle j | \kappa^{-1} | S\rangle, \quad j \in CS. \tag{17}$$

The interpretation of a detrapping probability follows from a comparison with (11). The probability of detrapping from site j for an initial condition given by $|p(0)\rangle$ at $t=0$ is

$$(\mathbf{Q})_j \equiv -W_{D,j}\langle j | \kappa^{-1} | p(0)\rangle, \quad j \in CS, \tag{18}$$

and the detrapping probability from site j for an initial condition given by the transient, normalized ($\langle \mathbf{1} | T_k\rangle = 1$) state $|T_k\rangle$ is

$$(\mathbf{Q_T})_{jk} \equiv -W_{D,j}\langle j | \kappa^{-1} | T_k\rangle, \quad j,k \in CS. \tag{19}$$

It shall be noted that in the case of a single reaction center the corresponding detrapping probabilities $\widetilde{Q}$ and $\widetilde{Q}_T$ are approximately equal, the difference being solely due to the contribution of dissipation events described by k_{diss}. In the dissipationless limit, i.e., for $k_{\mathrm{diss}} \rightarrow 0$, all the conditional detrapping probabilities reduce to a single detrapping probability given in terms of the ratio of total detrapping and charge transfer rates. With multiple reaction centers present, $(\mathbf{Q_T})_{ij}$ $(i \neq j)$ will, in general, be significantly smaller than $(\mathbf{Q_T})_{ii}$, as seen in the case of the PSI trimer in the next section. However, the sums $\sum_{j \in CS}(\mathbf{Q})_j$ and $\sum_{j \in CS}(\mathbf{Q_T})_{jk}$ become identical and equal to the overall detrapping probability in the dissipationless limit. This implies, in particular,

$$\sum_{j \in CS} (\mathbf{Q_T})_{jk} < 1, \quad \forall k \in CS. \tag{20}$$

Finally, let us introduce the sojourn time $(\mathbf{T}_{\mathrm{soj}})_j$ for charge separation site j defined as the average lifetime after a detrapping event at site j, but not involving any further detrapping events,

$$(\mathbf{T}_{\mathrm{soj}})_j = -\langle \mathbf{1} | \kappa^{-1} | T_j\rangle, \quad j \in CS. \tag{21}$$

For a system with only one charge separation site, the sojourn time is a measure of the time it takes for the excitation to leave and to return, i.e., to sojourn, to the reaction center. In a system with multiple reaction centers $(\mathbf{T}_{\mathrm{soj}})_j$ also includes processes where the excitation returns to another reaction center.

TABLE I. Quantities characterizing the sojourn expansion for trimeric PSI. The first usage time τ_0 denotes the average excitation lifetime without any detrapping events. The sojourn time $(\mathbf{T}_{soj})_i$ is the average lifetime for a transient state $|T_i\rangle$ immediately following detrapping at the charge transfer site i without any further detrapping events, whereas the corresponding detrapping probabilities are given by $(\mathbf{Q})_i$ in the case of initial condition $|p(0)\rangle$ and $(\mathbf{Q_T})_{ij}$ in the case of an initial condition corresponding to the transient state $|T_j\rangle$ following detrapping at site j. The quantity $3(\mathbf{Q})_i$ is the total detrapping probability for trimeric PSI. Because of the symmetry of the trimer, coefficients are identical for permuted site labels [see Eqs. (25) and (26)]. q is the quantum yield of the system. The decomposition of the average excitation lifetime is given in Eqs. (24) and (27).

τ	τ_0	$(\mathbf{T}_{soj})_i$	$(\mathbf{Q})_i$	$(\mathbf{Q_T})_{11}$	$(\mathbf{Q_T})_{12}$	$(\mathbf{Q_T})_{13}$	q
31.9 ps	18.9 ps	7.5 ps	21.0%	56.3%	3.7%	3.7%	0.968

Using Eqs. (18), (19), and (21) one can rewrite the terms of the expansion (16) as

$$\tau_1 = \mathbf{T}_{soj} \cdot \mathbf{Q},$$
$$\tau_2 = \mathbf{T}_{soj} \cdot \mathbf{Q_T} \cdot \mathbf{Q}, \qquad (22)$$
$$\tau_3 = \mathbf{T}_{soj} \cdot \mathbf{Q_T}^2 \cdot \mathbf{Q}.$$

The terms $\mathbf{T}_{soj}$ and $\mathbf{Q}$ are vectors of dimension M, and $\mathbf{Q_T}$ is an $M \times M$ matrix, where M is the number of charge separation sites in the system (i.e., $M=3$ for trimeric PSI with only one electron transfer branch assumed to be active in each reaction center core). This formulation significantly simplifies the expansion, as the terms of the expansion (16) involve products of matrices and vectors of size n (288 for the PSI trimer), while those of (22) are of size M (3 for the PSI trimer).

Convergence of the expansion defined by (16) and (22) can be proved by noting that any eigenvalue λ of $\mathbf{Q_T}$ satisfies $|\lambda| < 1$. If $\Sigma_j (\mathbf{Q_T})_{ij} x_j = \lambda x_i$, then it follows

$$|\lambda| \sum_i |x_i| = \sum_i |\lambda x_i|$$
$$= \sum_i \left| \sum_j (\mathbf{Q_T})_{ij} x_j \right| \leqslant \sum_i \sum_j |(\mathbf{Q_T})_{ij} x_j|$$
$$= \sum_j \left(\sum_i (\mathbf{Q_T})_{ij} \right) |x_j| < \sum_j |x_j|, \qquad (23)$$

where we have used (20) and the fact that the matrix elements $(\mathbf{Q_T})_{ij}$ are non-negative. Thus, $|\lambda| < 1$ and the sojourn expansion converges.

Since the sojourn expansion converges, the terms in (22) can be summed up to yield

$$\tau = \tau_0 + \mathbf{T}_{soj} \cdot (\mathbf{1}_M - \mathbf{Q_T})^{-1} \cdot \mathbf{Q}, \qquad (24)$$

where $\mathbf{1}_M$ denotes the identity matrix of dimension M. Equation (24) is a closed and exact expression for the average excitation lifetime in terms of the first usage time, the conditional detrapping probabilities and sojourn times.

IV. SOJOURN EXPANSION FOR EXCITATION MIGRATION IN TRIMERIC PSI

In this section we apply the expansion method developed in the preceding section to trimeric PSI. Due to the symmetry of the PSI trimer the expansion can be simplified. Below we will assume a uniform initial condition $|p(0)\rangle$, where each chlorophyll is equally likely to be excited.

The expansion terms (18), (19), and (21) introduced in the preceding section are invariant under a cyclic permutation of the indices of the charge transfer sites. Therefore, the sojourn times and the initial detrapping probabilities are identical for all three charge separation sites

$$(\mathbf{T}_{soj})_1 = (\mathbf{T}_{soj})_2 = (\mathbf{T}_{soj})_3,$$
$$(\mathbf{Q})_1 = (\mathbf{Q})_2 = (\mathbf{Q})_3. \qquad (25)$$

Furthermore, we have for the subsequent detrapping probabilities

$$(\mathbf{Q_T})_{11} = (\mathbf{Q_T})_{22} = (\mathbf{Q_T})_{33},$$
$$(\mathbf{Q_T})_{12} = (\mathbf{Q_T})_{23} = (\mathbf{Q_T})_{31}, \qquad (26)$$
$$(\mathbf{Q_T})_{21} = (\mathbf{Q_T})_{32} = (\mathbf{Q_T})_{13}.$$

The sojourn expansion (24) for trimeric PSI can be expressed in terms of the scalar quantities in Eqs. (25) and (26), as well as τ_0. One obtains

$$\tau = \tau_0 + 3(\mathbf{Q})_1 (\mathbf{T}_{soj})_1 / (1 - (\mathbf{Q_T})_{11} - (\mathbf{Q_T})_{12} - (\mathbf{Q_T})_{13}). \qquad (27)$$

The scalars (times and probabilities) are provided in Table I. A closer examination of these quantities reveals much about the excitation migration process.

Comparing τ and τ_0 in Table I one can conclude that more than 40% of the total excitation lifetime stems from detrapping events. The chance for a first detrapping event to occur at any one of the reaction centers after the initial uniform excitation of the system is given by $(\mathbf{Q})_i = 21\%$. As discussed in the preceding section, the overall detrapping probability for any initial condition, given, for example, by the sums $(\mathbf{Q})_1 + (\mathbf{Q})_2 + (\mathbf{Q})_3 = 63.0\%$ or $(\mathbf{Q_T})_{1j} + (\mathbf{Q_T})_{2j} + (\mathbf{Q_T})_{3j} = 63.7\%$ are approximately equal and close to 64.2%, which is the detrapping probability for an excitation that has already arrived at P700. The overall detrapping probabilities would be exactly identical in the dissipationless limit. The sum $(\mathbf{Q})_1 + (\mathbf{Q})_2 + (\mathbf{Q})_3$ is slightly less than $(\mathbf{Q_T})_{1j} + (\mathbf{Q_T})_{2j} + (\mathbf{Q_T})_{3j}$ because it represents a somewhat longer average migration path (starting from $|p(0)\rangle$ and $|T_j\rangle$, respectively), thus experiencing a slightly higher chance for the excitation to be dissipated during its migration.

A comparison of the conditional detrapping probabilities $(\mathbf{Q_T})_{11} = 56.3\%$ (jump from $|1\rangle$ to $|T_1\rangle$ and return to $|1\rangle$) and $(\mathbf{Q_T})_{12} = 3.7\%$ (jump from $|1\rangle$ to $|T_1\rangle$ and return to $|N+1\rangle$, i.e., to the second reaction center) reveals that the transient state resulting from a detrapping event at a reaction

TABLE II. Quantities characterizing the sojourn expansion for monomeric PSI. Definitions of the various terms below are analogous to those in Table I. The nuances between this model and the one presented in Ref. 32 are explained in the text.

$\tilde{\tau}$	$\tilde{\tau}_0$	$\tilde{T}_{\text{soj}}$	$\tilde{Q}$	$\tilde{Q}_T$	$\tilde{q}$
32.1 ps	19.1 ps	7.5 ps	63.0%	63.7%	0.968

center is not as likely to migrate to and detrap from another reaction center. This must be contrasted with the results of the next section, however, which indicate significant energy transfer between monomers. Charge separation probability at a remote reaction center as averaged over a whole monomer is a better measure of the integral connectivity between monomers than the detrapping probability across different reaction centers.

The quantum yield q for the system is the probability that an excitation will cause charge separation at a reaction center as opposed to being dissipated. It can be shown that in a model with a uniform dissipation constant k_{diss} (as in the present case) the quantum yield q is related to the average excitation lifetime[32]

$$q = 1 - k_{\text{diss}}\tau. \tag{28}$$

The high quantum yield for the trimer of 0.968 is due partly to the separation of the dissipation (1 ns) and excitation transfer timescales (≈ 0.1 ps, cf. Ref. 32) and partly to the lower site energy of charge separation sites.

In Ref. 32 we have reported a similar analysis of the excitation migration in the context of the sojourn expansion for the case of monomeric PSI. Before a comparison of those results with the ones for the PSI trimer presented here is performed, however, differences between the two models need to be noted. A discussion of how our current model is chosen is given in the introduction. In Ref. 32 both branches of the reaction center core were assumed to be active in charge separation. In order to simplify the formulation of the excitation migration in the context of the sojourn expansion, P700 was treated as a single unit, where thermal equilibration of excitation between two chlorophylls was assumed. Furthermore, a charge separation time of 1.5 ps was assumed in Ref. 32 as opposed to 1 ps in the present study.

To provide a comparison between the monomeric and trimeric excitation migration time scales we have performed a new analysis of the sojourn expansion in monomeric PSI. As shown in Ref. 32 the expansion yields

$$\tilde{\tau} = \tilde{\tau}_0 + \tilde{T}_{\text{soj}}\tilde{Q}/(1 - \tilde{Q}_T) \tag{29}$$

which, as expected, is analogous to expression (27) for the trimeric case. The quantities occurring in this expression are provided in Table II. The slight differences between the results in Table II and those reported in Ref. 32 reflect the aforementioned nuances between the two models. A comparison between the entries in Tables I and II reveals, not surprisingly, that the values of $\tau = 31.9$ ps^{-1} for the trimer and $\tilde{\tau} = 32.1$ ps^{-1} for the monomer are very close to each other. The connection between the monomers have little effect on the average excitation lifetime or the quantum yield.

This does not imply, however, that there is no significant energy transfer between individual monomers. We note that the mean lifetimes in Tables I and II are somewhat larger than the experimentally observed trapping times of about 20–25 ps.[19,22–26]

As mentioned in the Introduction, the questions regarding the directionality of charge transfer and which of the six chlorophylls performs the charge separation in PSI are currently unresolved. Alternative charge separation scenarios have been suggested for *Chlamydomonas*[45–47,62] Recent experiments revealed species specific differences in the physical chemical, e.g. spectroscopic, properties of P700;[63] the researchers studied the influence of nonconserved amino acid residues by site-directed mutagenesis of PSI from *Chlamydomonas*. The differences observed indicate that the differences in the amino acid sequences between cyanobacteria and green algae induce a significant shift in the site energies of the chlorophylls in *Chlamydomonas*.

In addition to the model described above, we have also considered the possibility of the charge separation starting from the P700 B-branch chlorophyll (eC-B1, corresponding to chlorophyll number 2) or the accessory chlorophyll on the B-branch (eC-A2, corresponding to chlorophyll number 4). The latter scenario was taken into account, because of the evidence provided in the recent work of Müller *et al.*[62] that charge separation may be initiated by the accessory chlorophyll on the B-branch.

The results described above do not change significantly when the model is altered to include two charge transfer sites (eC-A1 and eC-B1) per reaction center core as opposed to one (eC-A1). The average excitation lifetime and the quantum yield become 27.9 ps and 0.972, respectively, in such a scenario. The difference between the two sets of values is relatively small since the effect of eC-B1 as an additional trap is small compared to the overall excitation migration time scale.

Much larger effects on the average excitation lifetime and quantum yield are observed when either eC-B1 or eC-A2 is assumed to be the sole site where charge separation starts. In the case of eC-B1 a quantum yield of 0.874 and a lifetime of 127 ps is observed, while the case of eC-A2 results in a quantum yield of 0.829 and a lifetime of 171 ps. These large lifetimes and the corresponding low yields are partly a consequence of the relatively high site energies[35] of these two chlorophylls. These two values for the lifetime for eC-B1 and eC-A2 scenarios are unacceptably high, leading us to believe, based on the assumption of the accuracy of the corresponding site energies, that they do not present feasible alternatives to a model in which eC-A1 (by itself or together with eC-B1) is a charge separation site. This might indicate that the differences between cyanobacteria and *Chlamydomonas* could extend to the nature of the active branches.

V. THE DEGREE OF CONNECTIVITY BETWEEN PSI MONOMERS

In this section we consider the question of how integrally connected each PSI monomer is with its neighbors. Does trimeric PSI function largely as three separate monomers or is there substantial excitation transfer between indi-
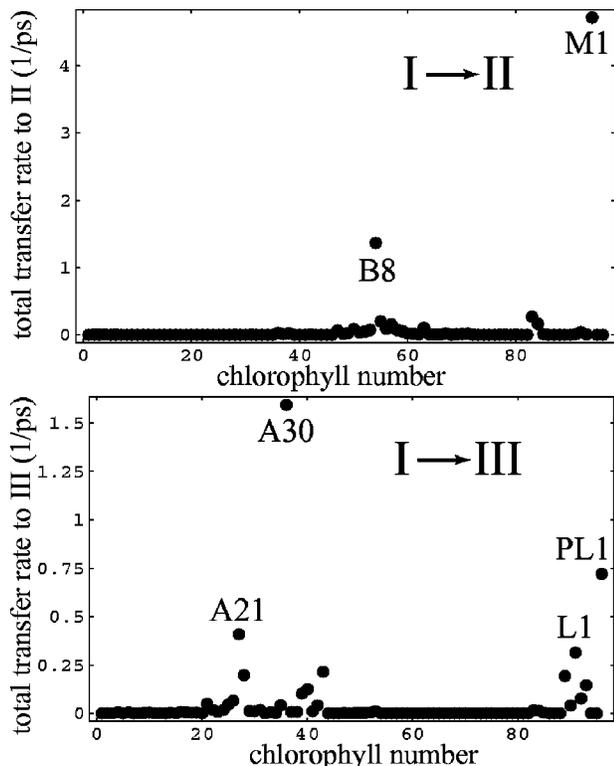
FIG. 2. Total rates of transfer from a given chlorophyll to a neighboring monomer. The monomers are labeled clockwise as I, II, and III with respect to the orientation given in Fig. 1. The chlorophylls with the highest transfer rates are highlighted (see also Table III and Fig. 3).

TABLE III. Chlorophylls with the highest transfer rates to neighboring monomers. Chlorophyll ID refers to the labels given in Ref. 9. Chlorophyll number refers to the ordering of chlorophylls in the corresponding PDB file 1JB0 (see also Figs. 2 and 3.) and resid is the residue ID of the same chlorophyll in the aforementioned structure file. The total transfer rate from chlorophyll i to a neighboring monomer is given by $\Sigma_j T_{ij}$, $j \in$ II or III. Percent rate indicates the percentage of the total transfer rate from the given chlorophyll to a monomer among all other chlorophylls.

Chl. ID	Chl. no.	resid	Total rate	Percent rate
		Transfer rates to monomer II		
M1	94	1601	4.7 ps^{-1}	59.9%
B8	54	1208	1.4 ps^{-1}	17.3%
		Transfer rates to monomer III		
A30	36	1130	1.6 ps^{-1}	34.3%
PL1	96	1801	0.72ps^{-1}	15.5%
A21	27	1121	0.41ps^{-1}	8.8%
L1	91	1501	0.31ps^{-1}	6.8%

A21, and L1 have the highest contributions to excitation transfer I→III. In fact, functionally M1 is essentially a part of the neighboring monomer. The total transfer rate from M1 in monomer I to monomer II is 4.7 ps^{-1}, while the corresponding rate to its own monomer is only 0.2 ps^{-1}. This is also apparent from the connectivity network portrayed in Fig. 3.

In this respect, it is also worth mentioning that PsaM (the protein subunit of PSI containing the boundary chlorophyll M1) is one of the two subunits that are specific to cyanobacteria[64] and is not present in plant PSI,[11] which has not been observed to form trimers. The function of PsaM may therefore be to provide additional protein-protein and protein-cofactor contacts between the monomers. It is astonishing that a chlorophyll that is coordinated by PsaM of one monomer functionally belongs to the neighboring monomer and shows tight hydrophobic interactions with the chlorophylls and carotenoids of that monomer; PsaM may be a major factor in the stabilization of the trimer as a whole.

B. Cross-monomer excitation trapping probabilities

The likelihood of an excitation initially at one monomer to be trapped eventually by its neighboring monomer provides a natural measure of the connectivity between two monomers. The trapping probability at reaction center RC_j for an initial state $|i\rangle$ localized at chlorophyll $i \in \{1,...,3N\}$, is given by [cf. Eq. (10)]

$$-k_{CS}\langle RC_j | K^{-1} | i \rangle. \tag{30}$$

The sum of these trapping probabilities over all reaction centers is equal to the quantum yield corresponding to an initial state $|i\rangle$.

The trapping probabilities as given by Eq. (30) are depicted in Fig. 4 as well as in Fig. 1(c). Not surprisingly, an excitation is more likely to be trapped in the monomer it has started from, with the exception of chlorophyll M1 as discussed above. However, there is a substantial chance of about 40% (19.7% for II→I and 20.0% for III→I, respectively) that the excitation will be trapped by one of the two neighboring monomers. There is a slight asymmetry between

vidual monomers? The most natural measure of the connectivity between different monomers would be given by the probability of an excitation initially located at one monomer to be trapped by another monomer. Another, perhaps simpler, measure is given by the total rate of transfer to neighboring monomers for chlorophylls along the intermonomer boundary. We will first examine these strongest connection points between monomers. In the latter half of this section we present an analysis of cross-monomer excitation trapping probabilities.

A. Intermonomer excitation transfer rates

The total rates of transfer from a chlorophyll $i \in$ I, in monomer I, to either of the two neighboring monomers are given by $\Sigma_{j \in II} T_{ij}$ and $\Sigma_{j \in III} T_{ij}$, respectively. In the following we will adopt a labelling of the individual monomers as given in Fig. 1 in a clockwise manner. Figure 2 presents total transfer rates to neighboring monomers across all 96 chlorophylls of a given monomer. Naturally, only chlorophylls close to the boundary contribute significantly to intermonomer excitation transfer. As a point of comparison, the average rate of transfer from a given chlorophyll to its own monomer is 14.1 ps^{-1}, while the *total* (not average) transfer rates from one monomer to another are 7.9 ps^{-1} for I→II and 4.6 ps^{-1} for I→III.

Chlorophylls with the highest transfer rates to neighboring monomers are listed in Table III and their relative positions are depicted in Fig. 3. The chlorophylls M1 and B8 are most prevalent in excitation transfer I→II, while A30, PL1,
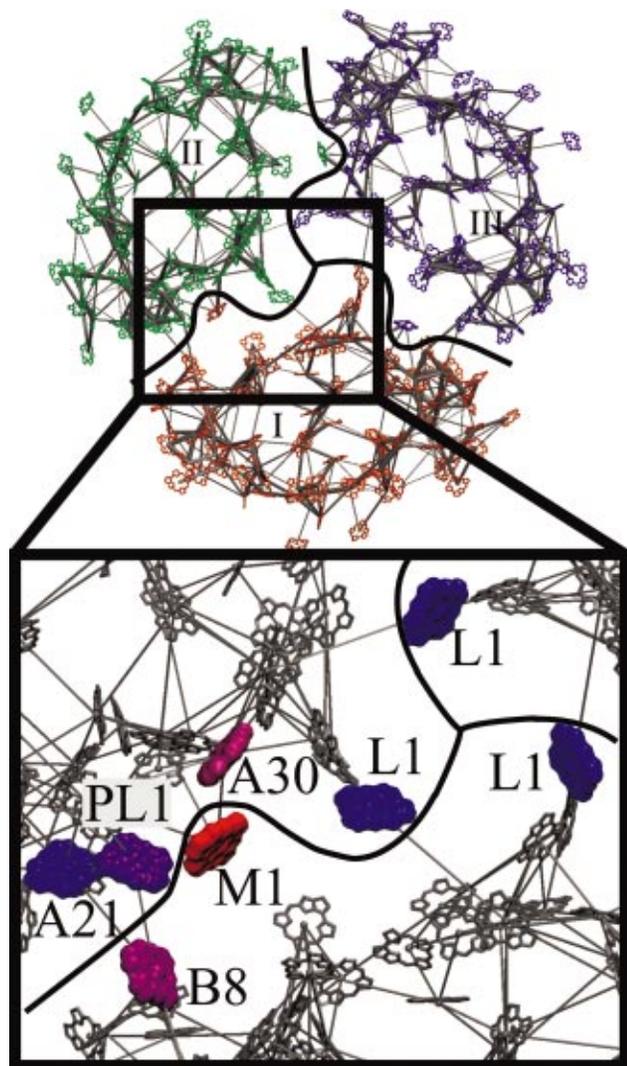
FIG. 3. (Color) Close-up view of the connection between neighboring monomers. Only the largest excitation transfer rates are indicated. The chlorophylls with the highest rates of transfer to neighboring monomers, as listed in Fig. 2 and Table III, are highlighted in color from blue to red in order of increasing transfer rate. Chlorophyll M1 is more strongly connected to the chlorophylls of the neighboring monomer than to those of its own monomer, being functionally part of the neighboring monomer. Figure produced with VMD (Ref. 57).
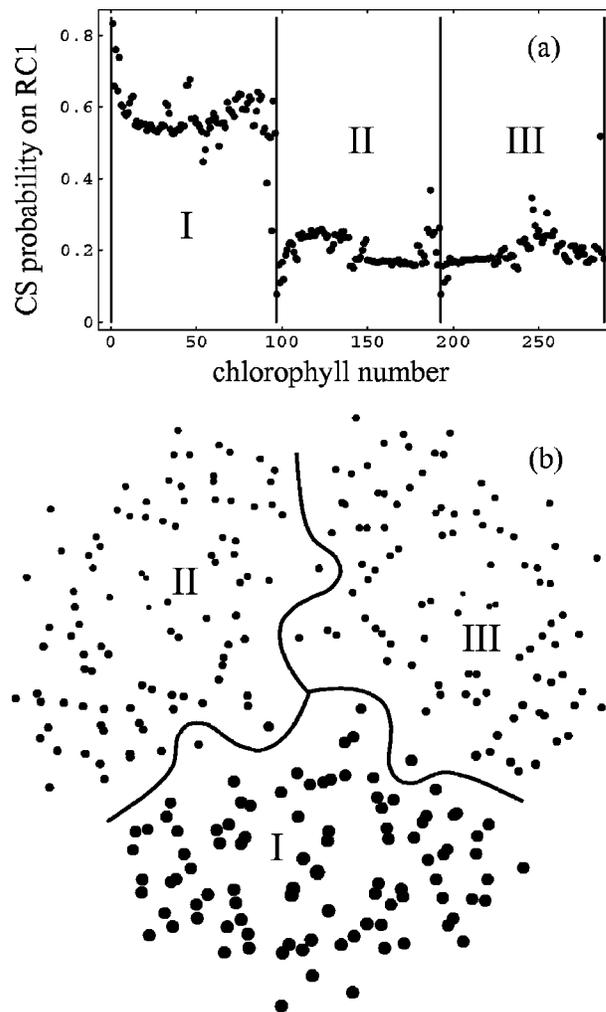

FIG. 4. Connectivity between PSI monomers. A measure of connectivity is given by the probability, calculated according to Eq. (30), of charge separation at the reaction center of another monomer for an initial state localized at a given chlorophyll. (a) Probabilities for charge separation at reaction center I as a function of chlorophyll number. The ordering used is identical to the one in the PDB file 1JB0 containing the structure (Ref. 9). Monomers I, II, and III are at the bottom, left, and right, respectively. Chlorophylls 1, 97, and 193 are the corresponding charge separation sites. The average of the charge separation probability at the reaction center of monomer I is 57.2% over monomer I, 19.7% over monomer II, and 20.0% over monomer III. (b) Probabilities for charge separation at reaction center I as a function of chlorophyll location. The probabilities are given by the area of each disk rendered proportional to the charge separation probability of that chlorophyll as also given in (a) [see Fig. 1(c) for a red–green–blue overlay of these probabilities for the three separate reaction centers].

migration probabilities to the left and the right neighbors. Naturally, the lowest probabilities for charge separation at reaction center I (7.8%) correspond to the case of the excitation initially starting from one of the two other reaction centers.

VI. ROBUSTNESS AND OPTIMALITY OF PSI CHLOROPHYLL NETWORK

Robustness of a system is a measure of its ability to cope with change. This is typically manifested in the form of a parameter insensitivity, as well as a tendency for graceful degradation. Optimality, on the other hand, is a measure of efficiency under a given set of constraints. For a typical light harvesting system, the fitness landscape over which the robustness and optimality should be judged is enormously complex and includes aspects of excitation migration, charge transfer, and photoprotection,[65] as well as synthesis, assembly, aggregation, repair, and regulation of the involved macromolecules. A comprehensive model including all these aspects is seemingly unattainable, although it is desirable to at least distinguish rate limiting steps from lesser constraints on the light harvesting function.

A simple, if somewhat restricted, measure for judging the robustness and optimality of a light harvesting system is the efficiency of the excitation migration process as given by the quantum yield evaluated according to Eq. (28). An earlier investigation within this context has been presented for the chlorophyll network of monomeric PSI.[32] A form of parameter insensitivity was seen by observing that thermal fluctua-
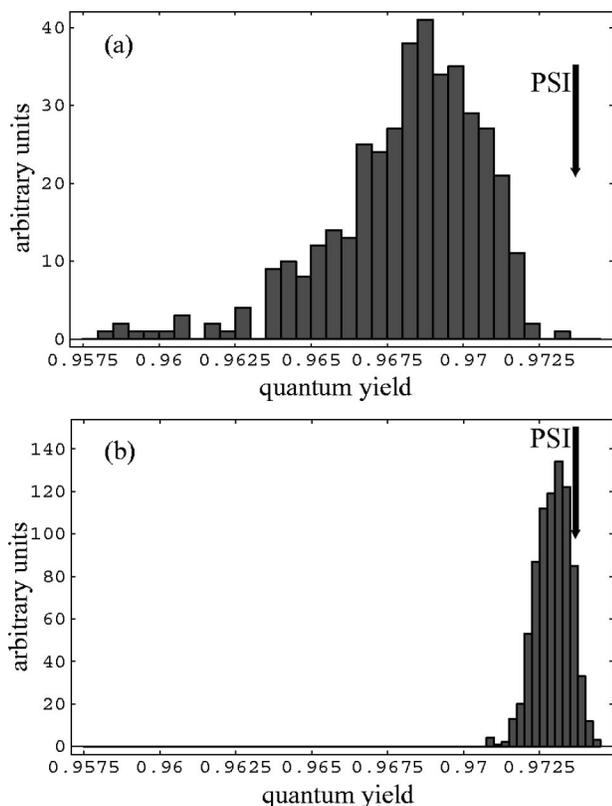
FIG. 5. Optimality of the chlorophyll network in trimeric PSI. Histograms of quantum yields, evaluated according to Eq. (28), over an ensemble of chlorophyll arrangements obtained by random rotations of the original chlorophyll orientations are shown (a) for an ensemble where all chlorophylls, including the reaction center chlorophylls are randomly rotated (400 configurations); (b) for an ensemble where the six reaction center chlorophylls are kept fixed within each monomer following (Ref. 36) (800 configurations). The long tail in (a) representing suboptimal configurations is largely due to the fluctuations of the reaction center chlorophylls.
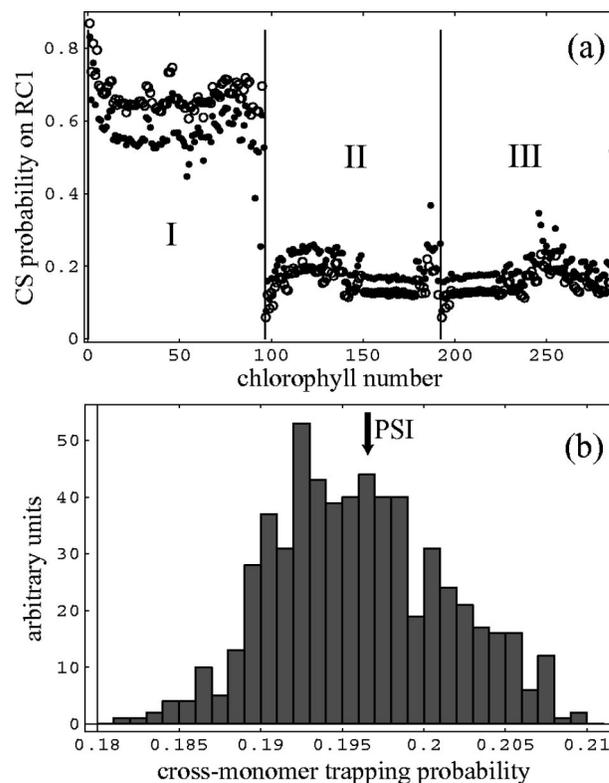

FIG. 6. Role of boundary chlorophylls in cross-monomer excitation migration. (a) Effect of pruning of the boundary chlorophylls, M1, B8, A30, PL1, A21, and L1, on cross-monomer trapping probabilities. Open circles represent the probabilities of charge separation at reaction center I for a given chlorophyll in a trimer without the aforementioned chlorophylls. For comparison they are overlayed with the original probabilities (points) as shown in Fig. 4(a). (b) Effect of random reorientation of boundary chlorophylls on cross-monomer trapping probabilities. The histogram displays the **I→II** cross-monomer trapping probabilities over an ensemble of 600 trimeric PSI-like chlorophyll networks, where only the aforementioned six boundary chlorophylls of each monomer were randomly reoriented. To reduce computational costs couplings of the aforementioned reoriented boundary chlorophylls to all other chlorophylls were computed in the dipole approximation, all other couplings are computed in the full Coulomb picture. The arrow indicates the probability corresponding to the original geometry (see caption of Fig. 4).

tions of chlorophyll site energies have little effect on the quantum yield at room temperature. This is a consequence of the broadness of chlorophyll absorption line shapes and no longer remains true at cryogenic temperatures, where the quantum yield drops significantly and becomes wavelength dependent. A sign of graceful degradation of the chlorophyll network was realized by noting that the pruning of individual chlorophylls from the network has little effect on the overall quantum yield beyond the loss of the corresponding cross section. The construction of an ensemble of PSI-like chlorophyll networks corresponding to random reorientations of chlorophyll molecules revealed, on the one hand, that the overall quantum yield changes only by a few percent across a wide ensemble, and on the other hand within that narrow distribution the original chlorophyll arrangement of PSI is near optimal. However, repeating random ensemble calculations by constraining the ensemble to one in which the six reaction center chlorophylls are held fixed in each monomer indicates that the apparent optimality is largely due to the orientations of the reaction center chlorophylls.[36] Distribution of quantum yields for trimeric PSI for ensembles with both constrained and unconstrained reaction center chlorophylls are presented in Fig. 5. The results are found to be similar to the case of monomeric PSI. It is seen that the

optimality of peripheral chlorophyll configurations are not as strongly pronounced as that of the central chlorophylls. It must be noted that the persistently large quantum yields reported in these studies are largely due to the separation of the dissipation and trapping time scales (1 ns versus 1 ps, respectively). Clearly, excitation migration does not contribute much to loss for the whole light harvesting process.

The existence of the trimeric form raises additional questions regarding the role and significance of individual chlorophylls in PSI, especially of the boundary chlorophylls discussed in the preceding section. The pruning of the six boundary chlorophylls, M1, B8, A30, PL1, A21, and L1, has a noticeable effect on cross-monomer trapping probabilities as shown in Fig. 6(a). The probability of an excitation that started in monomer I to be trapped at monomers I, II, and III, shift to 67.2%, 14.6%, and 15.1%, from 57.2%, 19.7%, and 20.0%, respectively, as a result of the pruning. Thus, the total cross-monomer trapping probability drops from 39.7% to 29.7%. However, the orientations of the aforementioned six

boundary chlorophylls seem not to be optimized for facilitating a maximal transfer between monomers as illustrated by the histogram in Fig. 6(b).

As a further point of comparison between the monomeric and trimeric forms, we have also examined the effect of massive pruning of chlorophylls (of up to 30% of the total number at the same time) on the quantum yield. It was seen that even this pruning to a high degree does not particularly favor the trimeric or the monomeric forms in terms of the overall quantum yield, as long as each individual monomer was assumed to contain a functioning reaction center.

We finally investigated the effect of a selective loss of reaction center function. The trimeric form, as opposed to separated monomers, has a chance to redirect excitation to another reaction center if one or two are dysfunctional. However, as long as a dysfunctional reaction center traps an excitation, no net quantum yield is gained by a trimeric arrangement. If the charge trapping ability is also lost, however, then quantum yields of 0.942 and 0.871 are maintained (with corresponding lifetimes of 58 ps and 129 ps), with the loss of one reaction center and two reaction centers, respectively, as opposed to loosing 1/3 and 2/3 of the total quantum yield outright in case of separated monomers.

VII. DISCUSSION

The rationale for the formation of trimeric PSI, as opposed to maintaining three separate monomers, is not immediately obvious. It may be explicable within the context of excitation migration, trapping, and subsequent charge transfer; trimeric PSI may have arisen because of better fault tolerance compared with the fault tolerance of individual monomers; trimer formation may also be an essential step in a further molecular assembly process. We have presented above an analysis of the excitation migration and trapping processes in the trimeric form of PSI to seek an explanation why cyanobacteria use trimeric PSI.

The total number of pigments per reaction center is identical in the trimeric and monomeric forms of PSI with the same subunit composition. As such, unlike in the case of the formation of iron stress-induced supercomplexes that add satellite proteins to a trimeric core, no obvious advantage is gained in terms of the absorption cross section per reaction center by going from three monomers to a trimer. A comparison of the bulk properties of excitation migration, such as quantum yield and average excitation lifetime, reveals similar results for monomeric and trimeric forms of PSI. Computations revealed an average excitation lifetime of 31.9 ps and a corresponding quantum yield of about 97%, changing only slightly between the monomeric and trimeric PSI forms.

Parameter sensitivity of the presented model must be considered before any conclusions can be drawn in earnest. We note that the computed value of an excitation lifetime of 31.9 ps reported here, as well as the slightly different values reported in Ref. 32, are longer than the experimentally reported values of about 20–25 ps. The quantitative details of the reported model depend on the site energies and couplings for the central chlorophylls as well as on the charge separation time scale; other parameters have a smaller effect on the model properties. We have assumed unidirectional charge

transfer, while other scenarios were also discussed. For a bidirectional model the computed average excitation lifetime becomes 27.9 ps.

Of great interest is the interconnectivity between individual monomers of a PSI trimer. As a first step in probing the interconnectivity, we have provided a framework for modelling the excitation migration in multireaction center, multicomponent light-harvesting systems. In particular, we have applied the sojourn expansion for the average excitation lifetime, which is based on expressing the excitation migration process in terms of detrapping and subsequent retrapping events. Our analysis revealed that detrapping and subsequent retrapping events contribute about 41% to the average excitation lifetime. The probability of a detrapped state to migrate to another reaction center is found to be much lower than the probability to migrate to the same reaction center.

As a further measure of the interconnectivity between monomers, we have identified the chlorophylls with the largest transfer rates to neighboring monomers. The chlorophyll M1 (cf., Fig. 3) is seen to be functionally a part of the next monomer. The transfer rates between monomers of 7.9 ps^{-1} and 4.6 ps^{-1} are small but nonnegligible with respect to the average detrapping rate of 14.1 ps^{-1} from a chlorophyll to its own monomer.

A more substantial measure of interconnectivity between monomers is the probability of an excitation initially at one monomer to be trapped at one of the two other monomers. We found this transfer of excitation from one monomer to another to be a frequent event. A substantial probability of about 40% is found for an excitation to be trapped by the two neighboring monomers. The pruning of the most influential six boundary chlorophylls is seen to reduce this cross-monomer trapping probability to about 30%.

In this regard, it is surprising that a comparison of the quantum yields reveals that no significant advantage is gained by the formation of trimeric PSI instead of maintaining three separate monomers. However, it is plausible that a small advantage for the trimer can yield a larger advantage in the race of the survival of the fittest under light-limiting conditions. Examples where competitive advantage are displayed even without any pronounced phenotypical differences have been observed in growth competition experiments.[66,67]

It is of interest to note that PSI is stabilized by trimer formation. PSI monomers, isolated from cyanobacteria are nonstable and the peripheral subunits (PsaL, PsaI, PsaM, and PsaK) as well as several chlorophylls and carotenoids are easily lost. The stabilization of the antenna system may also be an important function of the trimeric organization. However, these effects alone may be insufficient to explain the advantage of the trimerization. Further factors have to be taken into account, for example, the changes that cells undergo when shifted from medium to low light intensity. In this case, the cells rest for two to three days performing *de novo* synthesis of PSI. Whereas the majority of PSI is monomeric at medium light intensity, the newly synthesized PSI is trimeric. The ratio of PSI to PSII increases also from 1.5 to 8.[16] Furthermore, the cells increase the amount of phycobilli-

somes, acting as peripheral antenna. After this transition the cells start to grow with nearly the same doubling time as before at 10 times higher light intensity. Under low illumination conditions with 8 times more PSI than PSII, it is likely that cells get their energy supply mainly from cyclic electron transfer around PSI. The trimer may be necessary for the cyclic electron transport. Furthermore, significant amounts of the phycobillisomes are attached to PSI at low light intensity. Possibly the trimer is necessary for the interaction of PSI with phycobillisomes. Both of these hypotheses would explain the advantage of trimerization, however so far there is no experimental report that answers these questions.

From a theoretical perspective, an analysis of excitation migration presents a necessary first step. However, we find that the limited scope of an analysis based solely upon excitation transfer is insufficient to explain the behavior of the expression of trimeric *vs.* monomeric forms of PSI conclusively. A more elaborate study including the effects of wavelength dependence on the excitation migration process and other aspects of the light harvesting function such as charge transfer character seems to be necessary for unravelling the rationale of trimer formation in cyanobacterial PSI.

Finally, we would like to note that the methods developed here, especially the generalized sojourn expansion leading to the elegant and succinct final expression (24), can be readily applied to analyze the excitation migration processes in other multicomponent light harvesting systems, such as the iron stress-induced supercomplexes mentioned in the introduction or an elaborate model of the purple bacterial photosynthetic unit with multiple reaction centers and peripheral light harvesting complexes as soon as an effective Hamiltonian picture is constructed.

ACKNOWLEDGMENTS

[1] H. van Amerongen, L. Valkunas, and R. van Grondelle, *Photosynthetic Excitons* (World Scientific, Singapore, 2000).

[2] R. E. Blankenship, *Molecular Mechanisms of Photosynthesis* (Blackwell Science, Malden, MA, 2002).

[3] J. Xiong, W. M. Fischer, K. Inoue, M. Nakahara, and C. E. Bauer, Science **289**, 1724 (2000).

[4] R. E. Blankenship, Trends Plant Sci. **6**, 4 (2001).

[5] K. R. Miller, Nature (London) **300**, 53 (1982).

[6] G. McDermott, S. M. Prince, A. A. Freer, A. M. Hawthornthwaite-Lawless, M. Z. Papiz, R. J. Cogdell, and N. W. Isaacs, Nature (London) **374**, 517 (1995).

[7] J. Koepke, X. Hu, C. Muenke, K. Schulten, and H. Michel, J. Hematother **4**, 581 (1996).

[8] X. Hu, T. Ritz, A. Damjanović, and K. Schulten, J. Phys. Chem. B **101**, 3854 (1997).

[9] P. Jordan, P. Fromme, H. T. Witt, O. Klukas, W. Saenger, and N. Krauß, Nature (London) **411**, 909 (2001).

[10] A. Zouni, H.-T. Witt, J. Kern, P. Fromme, N. Krauss, W. Saenger, and P. Orth, Nature (London) **409**, 739 (2001).

[11] A. Ben-Shem, F. Frolow, and N. Nelson, Nature (London) **426**, 630 (2003).

[12] T. S. Bibby, J. Nield, and J. Barber, Nature (London) **412**, 743 (2001).

[13] T. S. Bibby, J. Nield, and J. Barber, J. Biol. Chem. **276**, 43246 (2001).

[14] E. J. Boekema, A. Hifney, A. E. Yakushevska, M. Piotrowski, W. Keeg-stra, S. Berry, K.-P. Michel, E. K. Pistorius, and J. Kruip, Nature (London) **412**, 745 (2003).

[15] T. S. Bibby, J. Nield, M. Chen, A. W. D. Larkum, and J. Barber, Proc. Natl. Acad. Sci. U.S.A. **100**, 9050 (2003).

[16] P. Fromme, *Crystallization of Photosystem I for Structural Analysis* (Habilitation, Technical University Berlin, Berlin, Germany, 1998).

[17] P. Fromme, S. Janson, and E. Schlodder, "Structure and function of the antenna system in photosystem I," in *Ligth Harvesting Antennas in Photosynthesis*, edited by B. Green and B. Parson (Kluwer Academic, Dordrecht, 2003), pp. 253–279.

[18] A. N. Melkozernov, T. S. Bibby, S. Lin, J. Barber, and R. E. Blankenship, Biochemistry **42**, 3893 (2003).

[19] A. R. Holzwarth, G. Schatz, H. Brock, and E. Bittersmann, Biophys. J. **64**, 1813 (1993).

[20] L. Valkunas, V. Liuola, J. P. Dekker, and R. van Grondelle, Photosyn. Res. **43**, 149 (1995).

[21] L.-O. Pålsson, C. Flemming, B. Gobets, R. van Grondelle, J. P. Dekker, and E. Schlodder, Biophys. J. **74**, 2611 (1998).

[22] A. N. Melkozernov, S. Lin, and R. E. Blankenship, J. Phys. Chem. B **104**, 1651 (2000).

[23] A. N. Melkozernov, S. Lin, and R. E. Blankenship, Biochemistry **39**, 1489 (2000).

[24] B. Gobets, I. H. M. van Stokkum, M. Rögner, J. Kruip, E. Schlodder, N. V. Karapetyan, J. P. Dekker, and R. van Grondelle, Biophys. J. **81**, 407 (2001).

[25] A. N. Melkozernov, S. Lin, R. E. Blankenship, and L. Valkunas, Biophys. J. **81**, 1144 (2001).

[26] J. T. M. Kennis, B. Gobets, I. H. M. van Stokkum, J. P. Dekker, R. van Grondelle, and G. R. Fleming, J. Phys. Chem. B **105**, 4485 (2001).

[27] V. Zazubovich, S. Matsuzaki, T. W. Johnson, J. M. Hayes, P. R. Chitnis, and G. J. Small, Chem. Phys. **275**, 47 (2002).

[28] B. Gobets and R. van Grondelle, Biochim. Biophys. Acta **1507**, 80 (2001).

[29] P. R. Chitnis, Annu. Rev. Plant Physiol. Plant Mol. Biol. **52**, 593 (2001).

[30] A. N. Melkozernov, Photosyn. Res. **70**, 129 (2001).

[31] M. Byrdin, P. Jordan, N. Krauß, P. Fromme, D. Stehlik, and E. Schlodder, Biophys. J. **83**, 433 (2002).

[32] M. K. Şener, D. Lu, T. Ritz, S. Park, P. Fromme, and K. Schulten, J. Phys. Chem. B **106**, 7948 (2002).

[33] X. Hu, T. Ritz, A. Damjanović, F. Autenrieth, and K. Schulten, Q. Rev. Biophys. **35**, 1 (2002).

[34] T. Ritz, A. Damjanović, and K. Schulten, ChemPhysChem **3**, 243 (2002).

[35] A. Damjanovic, H. M. Vaswani, P. Fromme, and G. R. Fleming, J. Phys. Chem. B **106**, 10251 (2002).

[36] M. Yang, A. Damjanović, H. M. Vaswani, and G. R. Fleming, Biophys. J. **85**, 140 (2003).

[37] M. Yang and G. R. Fleming, Chem. Phys. **282**, 163 (2002).

[38] M. Yang and G. R. Fleming, J. Chem. Phys. **119**, 5614 (2003).

[39] E. G. Alexov and M. R. Gunner, Biochemistry **38**, 8253 (1999).

[40] Q. Xu, L. Baciou, P. Sebban, and M. R. Gunner, Biochemistry **41**, 10021 (2002).

[41] Z. Katiliene, E. Katilius, and N. W. Woodbury, Biophys. J. **84**, 3240 (2003).

[42] F. Yang, G. Shen, W. M. Schluchter, B. L. Zybailov, A. O. Ganago, I. R. Vassiliev, D. A. Bryant, and J. H. Golbeck, J. Phys. Chem. B **102**, 8288 (1998).

[43] W. Xu, P. R. Chitnis, A. Valieva *et al.*, J. Biol. Chem. **278**, 27864 (2002).

[44] W. Xu, P. R. Chitnis, A. Valieva *et al.*, J. Biol. Chem. **278**, 27876 (2002).

[45] S. E. Rigby, I. P. Muhiuddin, M. C. Evans, S. Purton, and P. Heathcote, Biochim. Biophys. Acta **1556**, 13 (2002).

[46] W. V. Fairclough, A. Forsyth, M. C. Evans, S. E. Rigby, S. Purton, and P. Heathcote, Biochim. Biophys. Acta **1606**, 43 (2003).

[47] M. Guergova-Kuras, B. Boudreaux, A. Joliot, P. Joliot, and K. Redding, Proc. Natl. Acad. Sci. U.S.A. **98**, 4437 (2001).

[48] B. Gobets, L. Valkunas, and R. van Grondelle, Biophys. J. **85**, 3872 (2003).

[49] R. Zwanzig, *Nonequilibrium Statistical Mechanics* (Oxford University Press, New York, 2001).

[50] A. Damjanović, T. Ritz, and K. Schulten, Phys. Rev. E **59**, 3293 (1999).

[51] A. Damjanović, T. Ritz, and K. Schulten, Biophys. J. **79**, 1695 (2000).

[52] A. Damjanović, I. Kosztin, U. Kleinekathoefer, and K. Schulten, Phys. Rev. E **65**, 031919 (2002).

[53] T. Förster, Ann. Phys. (Leipzig) **2**, 55 (1948).

[54] D. L. Dexter, J. Chem. Phys. **21**, 836 (1953).

[55] T. Ritz, S. Park, and K. Schulten, J. Phys. Chem. B **105**, 8259 (2001).

[56] H. Scheer, *Chlorophylls* (CRC, Boca Raton, FL, 1991).

[57] W. Humphrey, A. Dalke, and K. Schulten, J. Mol. Graphics **14**, 33 (1996).

[58] T. G. Owens, S. P. Webb, L. Mets, R. S. Alberte, and G. R. Fleming, Proc. Natl. Acad. Sci. U.S.A. **84**, 1532 (1987).

[59] R. van Grondelle, J. P. Dekker, T. Gillbro, and V. Sundström, Biochim. Biophys. Acta **1187**, 1 (1994).

[60] K. Brettel, Biochim. Biophys. Acta **1318**, 322 (1997).

[61] S. Park, M. K. Şener, D. Lu, and K. Schulten, J. Chem. Phys. **119**, 1313 (2003).

[62] M. G. Müller, J. Niklas, W. Lubitz, and A. R. Holzwarth, Biophys. J. **85**, 3899 (2003).

[63] H. Witt, E. Bordignon, D. Carbonera, J. P. Dekker, N. V. Karapetyan, C. Teutloff, A. Webber, W. Lubitz, and E. Schlodder, J. Biol. Chem. **278**, 46760 (2003).

[64] U. Mühlenhoff, W. Haehnel, H. T. Witt, and R. G. Herrmann, Gene **127**, 71 (1993).

[65] A. J. Young and H. A. Frank, Photochem. Photobiol. **36**, 3 (1996).

[66] Y. Ouyang, C. R. Andersson, T. Kondo, S. S. Golden, and C. H. Johnson, Proc. Natl. Acad. Sci. U.S.A. **95**, 8660 (1998).

[67] D. Gonze, M. R. Roussel, and A. Goldbeter, J. Theor. Biol. **214**, 577 (2002).